

## CHAPTER 3

# Can Building Footprint Extraction from LiDAR be Used Productively in a Topographic Mapping Context?

Carol Agius and James Brearley

### Introduction

Light Detection and Ranging (LiDAR) is a quick and economical method for obtaining cloud-point data that can be used in various disciplines and a diversity of applications. LiDAR is a technique that is based on laser technology. The process looks at the two-way travel time of laser beams and measures the time and distance travelled between the laser sensor and the ground (Shan & Sampath, 2005). National Mapping Agencies (NMAs) have traditionally relied on manual methods, such as photogrammetric capture, to collect topographic detail. These methods are laborious, work-intensive, lengthy and hence, costly. In addition because photogrammetric capture methods are often time-consuming, by the time the capture has been carried out, the information source, that is the aerial photography, is out of date (Jenson and Cowen, 1999). Hence NMAs aspire to exploit methods of data capture that are efficient, quick, and cost-effective while producing high quality outputs, which is why the application of LiDAR within NMAs has been increasing.

One application that has seen significant advances in the last decade is building footprint extraction (Shirowzhan and Lim, 2013). The buildings layer is a key reference dataset and having up-to-date, current and complete building information is of paramount importance, as can be witnessed with government agencies and the private sectors spending millions each year on aerial photography as a source for collecting building footprint information (Jenson and Cowen, 1999). In the last decade automatic extraction of building footprints from LiDAR data has improved sufficiently to be of an acceptable accuracy for urban planning (Shirowzhan and Lim, 2013).

The most common and cost-effective outputs from LiDAR are Digital Surface Models (DSMs) and Digital Terrain Models (DTMs) (Priestnall et al., 2000). However it would be useful to use LiDAR to generate other outputs, such as building footprints. Although, research does indicate that the automatic detection of buildings has not yet been fully achieved (Awrangjeb et al., 2010) there is the hope in the future that the building footprints created from LiDAR data can be added to the large-scale basemaps. This is due to the fact

that building capture using photogrammetric means is often labour intensive.

Digital Surface Models are very useful at providing building locations, and LiDAR in recent times has been considered as a cost effective and accurate method of creating DSMs (Hill et al., 2000). The creation of DSMs and DTMs can be seen as the first inputs into one method for building extraction by subtracting the DSMs away from the DTMs. This process retains features above the terrain, such as buildings and vegetation. The process can be refined by filtering the resulting data on a height threshold to remove vegetation and other anomalies (Haithcoat et al., 2001; Kwak & Habib, 2013). Bayesian Network Classification can be used to detect buildings based on the height difference between DSMs and DEMs (Ma, 2005). The rationale for this method is the assumption that separate surface features from ground elevation data are higher than the features from the surrounding surface (Priestnall et al., 2000). The Bayesian approach has been attempted to extract building footprint solely from LiDAR data whilst also attempting to retain the highest possible accuracy (Wang et al, 2006). Other methods have been tried for extracting building footprints from LiDAR.

The extraction of building footprints is often attempted by four steps that are often seen as successful: differentiating between ground and non ground points, identifying building features, determining building footprints and finally, generalising footprint boundaries (Kim & Shan, 2011). Some other current building extraction methods are attempting the use of Triangular Irregular Networks (TINs) polygons to be able to classify the buildings for the extraction (Alexander et al., 2009). These TIN polygons are also used to help with the separation of buildings and vegetation based on the height difference. The use of TINs to categorise building was shown to be especially effective when there is a sudden change within elevation between the data (Alexander et al., 2008).

A morphological filter is often implemented to distinguish between terrain and non-terrain segments, and is viewed as a core action for building extraction (Elashker & Bethel, 2002). Once the original data has been filtered Shiravi et al. (2012) recommend trying various assessments by adding the height data to check that the buildings fit the requirements. These would be expected to give a high accuracy for building footprints from LiDAR data. In fact the dataset produced sometimes has more accurate height values than it does boundary lines, with water sometimes causing anomalies with the data recorded (Awrangzeb et al., 2010). Another issue with building footprint extraction from LiDAR arises when certain aspects are not always correctly removed because of 'debris' or small buildings being left over from the extraction process (Kim & Shan, 2011). A different problem is holes within buildings and that closed polygons cannot be identified automatically (Shirowzhan & Lim, 2013). Vegetation is an additional problem when extracting building footprints from LiDAR data because vegetation and trees 'interfere' with the urban features, so selection and removal of these features, especially in the pre-

processing stages is recommended (Zhou & Neuman, 2013). Various authors suggest using intensity values to identify vegetation features, distinguishing the vegetation from buildings and terrain will facilitate the separation of the data (Thuy Vu, 2009; Goepfer et al., 2008).

### **Methodology**

The LiDAR data acquired through the ERDF 156 project has a point density of 0.25 meters and the cloud points were classified into three categories: ground, unassigned, and water. The scope of the exercise was to investigate how the point cloud data could be manipulated to extract building footprints. Comparing the resulting dataset with the existing buildings data captured photogrammetrically and orthophoto maps generated from aerial photography shot at the same time as the LiDAR survey will highlight and detect changes. The trials were carried out to investigate whether the LiDAR extracted data can potentially be used as a stop-gap to temporarily update the building features on existing large-scale basemaps until the missing features can be captured photogrammetrically from aerial photography.

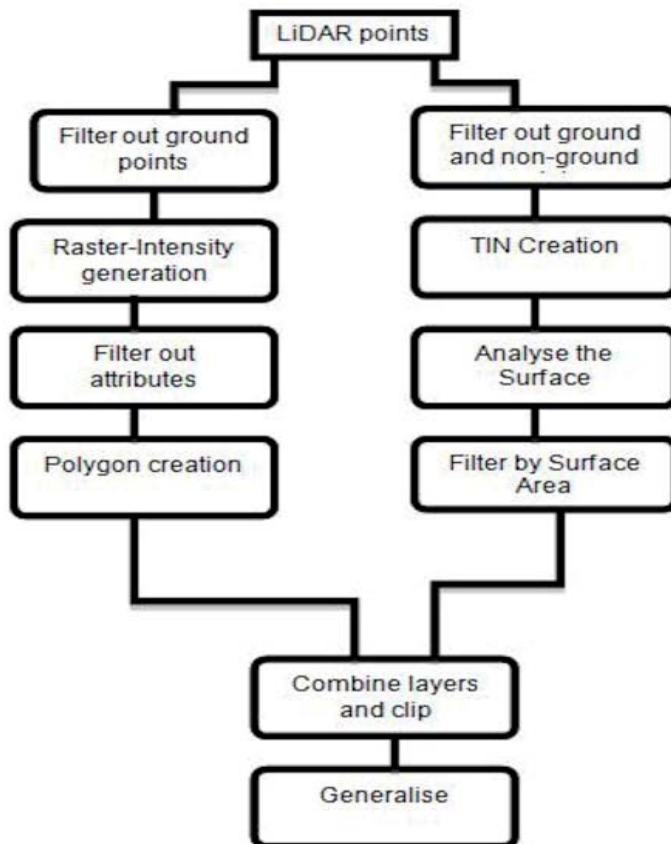
In order to extract the building footprints the method adopted was broken down into a number of different stages. The techniques used were not based on the specific methods researched from previous work and studies; however the research provided an understanding of potential approaches to implement to achieve the desired objective. The LiDAR point cloud data was supplied in 1km x 1km tiles. Tiles in three sites were selected for the trials, the selection was based on the terrain, topographic content and the height variations of the built environment:

- Tigne Point in Sliema – dense urban coastal area with great variation in building heights ranging from 2 to 15 stories, with minimal ground urban vegetation and roof top gardens;
- Il-Maqluba in Gudja – undulating terrain, including a doeline, showing mixed urban and rural area typically depicting terraced fields bounded with thick rubble walls;
- Mosta – urban fabric of mostly homogenous building heights with adjacent watercourse valley and both natural and structured urbanised vegetation.

As mentioned previously, the supplied LiDAR point cloud data was only classified into three categories: water, ground and unassigned. This meant that the unassigned category contained return data from buildings, vegetation, boats, vehicles, walls, power cables, and cranes besides other 'noise'. The aim of the approaches adopted was to filter out just the building data from all the above-ground information captured by the LiDAR survey. The desired end result was building footprints, so the goal was to extract the outlines of the

building features rather than their heights above ground. The process flow line was two-pronged. Process 1 was based on polygon outlines generated on the intensity values of the LiDAR returns. Process 2 was based on analysing the surface differences of Triangulated Irregular Networks (TINs) derived from the elevation of the LiDAR data. The results were then compared against each other to extract the building outlines.

Figure 1: Process flow line



### *Process 1*

Process 1 focused on the intensity values of the LiDAR data and aimed to filter buildings based on their intensity values. The process entailed the following steps:

- Filter out ground points

The LiDAR data were supplied categorised in three classifications. For the first step of Process 1 the points for each of the trial areas categorised as ‘unassigned’ were selected from the point cloud data. The unassigned points were first returns from above ground features, which excluded roads, rock surfaces, soil and other ground-level surfaces.

-Raster Intensity Generation

A raster map based on the intensity values of the LiDAR returns was generated on the points categorised as unassigned. The values of different features on the resulting intensity raster maps were noted and compared to each other; these features included buildings, vegetation, vehicles and other features.

-Filter out on the intensity attributes

In the local context it was observed that vegetation has lower intensity values compared to the buildings which often have higher intensity values; due to the reflectance values that are returned from vegetation features. Therefore filtering these lower values out removed the vegetation from the raster, leaving behind the points returned from building and vehicles which can be filtered out at a later date following further processing. One issue that arose from this process was that the difference in intensity values between buildings and vegetation was more marked in urban areas than in rural areas. This was due to the urban vegetation being ‘greener’, possibly from better irrigation compared to the more arid rural areas. In rural areas the intensity filtering also picked up rubble walls since these are composed of the same fabric as buildings.

- Polygon creation

The filtering out based on intensity attributes produced raster maps which were polygonised using standard software tools.

Figure 2: Mosta - Filtered intensity map depicting buildings and vehicles



### ***Process 2***

Process 2 focused on filtering the data based on height values. Rather than work with DEMs and DSMs this study opted to work with Triangulated Irregular Networks since TINs retain information such as surface area, volume, etc.

- Filter out ground and non-ground points

In Process 2 two point files for each of the trial areas were created. The first was the raw LiDAR point cloud data, all returns and all classifications. The second was the all returns of the points categorised as 'unassigned'.

- TIN Creation

Two TINs were then created; the first of the unfiltered LiDAR points all returns and all classifications shown in Figure 3 below. The second TIN was generated from all returns of the non-ground, unassigned points shown in Figure 4.

- Analyse the Surface Difference

The resulting two TINs were then compared against each other to determine the surface difference between the ground points and the above-ground points. The end result was a dataset of polygons depicting above ground features which included buildings, vegetation, cars, field boundaries and buses. An example of the output is shown in Figure 5 below.

- Filter by Surface Area

Using area as a filter it is possible to eliminate objects that are much smaller than buildings, such cars and small field boundaries.

Figure 3: Mosta – TIN of all LiDAR returns all classifications

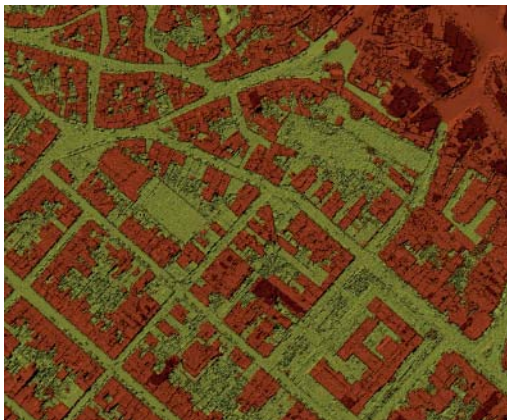


Figure 4: Mosta - TIN of all LiDAR returns 'unassigned'

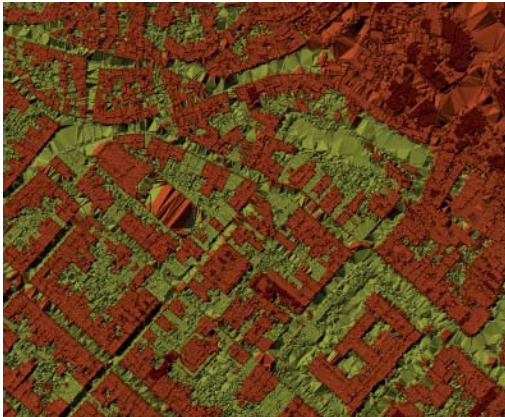
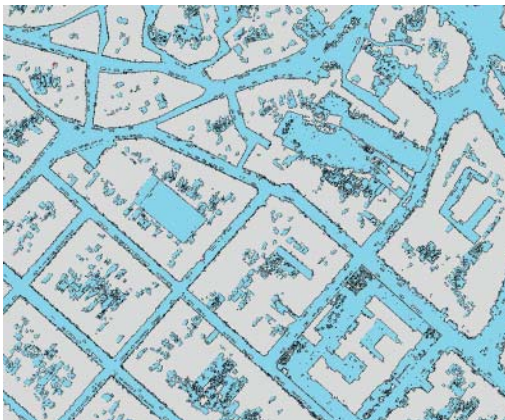


Figure 5: Surface difference between unassigned TIN and all classifications TIN



#### - Combining of TINs and Intensity Results

Once both processes were finalised the next step was to combine the results. Process 1, based on intensity filtering, produced a polygon dataset that contained buildings and vehicles but eliminated vegetation. Process 2 produced a polygon dataset that contained buildings and vegetation but eliminated all but the largest vehicles, example buses, and overhead cranes. The next step was to compare the two results against each other and remove the polygons that do not overlap. Only the common areas in both outputs were retained eliminating features that were not present. This resulted in the clean removal of

both the vegetation and vehicles that would have been previously left behind should only one of the filtering methods have been used in isolation rather than in combination. This was largely successful, especially in the more developed areas such as Silema.

#### - Generalisation

The previous step resulted in a fairly clear selection of building footprints. However, it was still necessary to carry out generalisation and smoothing to tidy any gaps in the buildings from where points were never assigned during the aerial survey. These processes also simplified the building footprints, making them more aesthetically pleasing.

Figure 6: Mosta - Resulting output building footprints after generalisation and smoothing



## Results

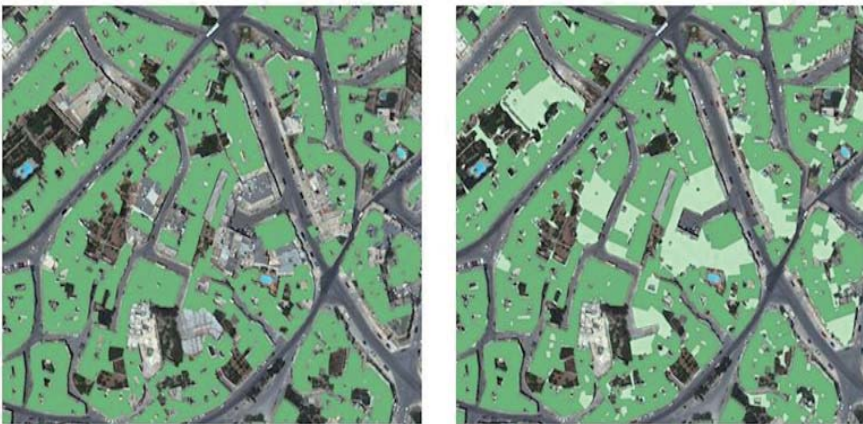
The results from the three trials were examined to establish the quality of outputs and determine whether the data can be used productively. The outputs of all the three trial areas were compared with aerial imagery acquired in the same period as the LiDAR survey and against a buildings vector dataset acquired through photogrammetric capture from older low-flying aerial photography. The aims of the comparison were to investigate whether the polygons extracted did constitute a complete buildings dataset without either omitting building features or 'inventing' building polygons. The comparison was also useful to verify the positional accuracy and the shape of the building polygons extracted from LiDAR.

Spatiotemporal analysis of the LiDAR extracted building footprints against the older photogrammetrically captured building blocks was then carried out. The building footprints extracted from LiDAR were overlaid over the building footprints captured photogrammetrically in order to identify any polygons present in the LiDAR footprints but



not in the existing buildings layer. In theory these ‘new’ polygons represent changes in the buildings dataset since the last aerial photography, in other words new development on the ground that needs to be updated in the buildings dataset. The comparisons did highlight substantial development changes to the urban areas since the previous photogrammetric capture. In order to verify the authenticity of this assumption the highlighted polygons were compared against orthophotos produced from aerial photography shot in the same period as the LiDAR survey. The visual comparison backed up the assumption and verified that the ‘new’ polygons are indeed new building features present on the orthophoto and missing from the current buildings dataset. These changes are most likely due to the development of the areas since the previous photogrammetric capture had taken place.

Figure 7: Mosta showing photogrammetrically captured buildings over an orthophoto (left), and the change in development detected by LiDAR footprint extraction (right)



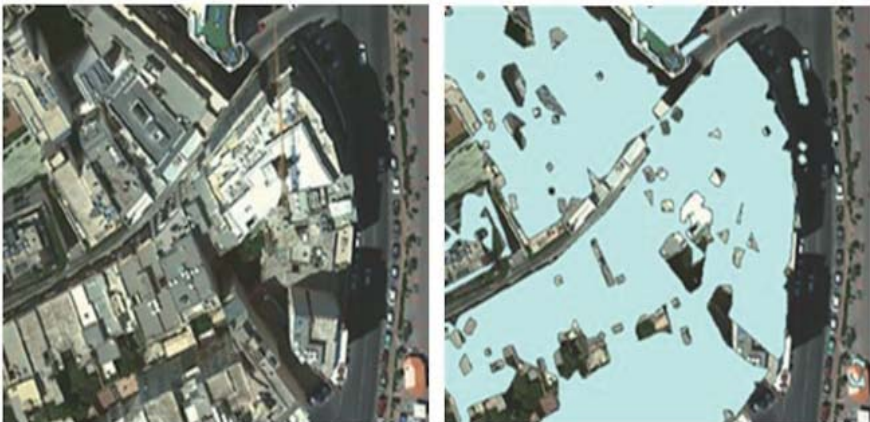
Positional accuracy is a measure of how closely the points in a dataset agree with the corresponding points in the real world. In large-scale topographic mapping at scales of 1:1250 typical positional accuracy is of  $<\pm 1.0\text{m}$  (OS, 2005). The building footprints extracted from LiDAR were compared with the photogrammetrically captured building footprints and tested for positional accuracy; the results ranged from  $\pm 1.2\text{m}$  to  $\pm 1.5\text{m}$ , which are fair results. However it should be noted that the tests were carried out on a large-scale dataset not on ground survey data, so the positional accuracy of the results is less and cannot be deemed sufficient for scales greater than 1:2500. This indicates that the LiDAR building footprints cannot be used to update directly to the current large-scale data, which is 1:1000 scale, without necessitating considerable manual editing and manipulation.

Building shape is one aspect that suffered from the extraction process. The most noticeable is the number of 'holes' generated in the building polygons from the extraction process. These require further work to eliminate. Another issue that compromised the shape of the extracted building outlines where protruding balconies and terraces. These not only created jagged edges which required smoothing but also distorted the shape by extending the building outline further than the actual footprint itself.

Figure 8: Sliema showing how protruding balconies extend the building outlines further than actual footprint, and superfluous 'holes'



Figure 9: Sliema showing how buildings in close proximity are joined into one polygon



Simplifying, smoothing and buffering carried out on the dataset following the extraction process did introduce an element of distortion to the shape of the building footprints. In a few cases the process joined some close polygons together, this requires a certain amount of manual editing to correct. The final output also suffers from some round edges.

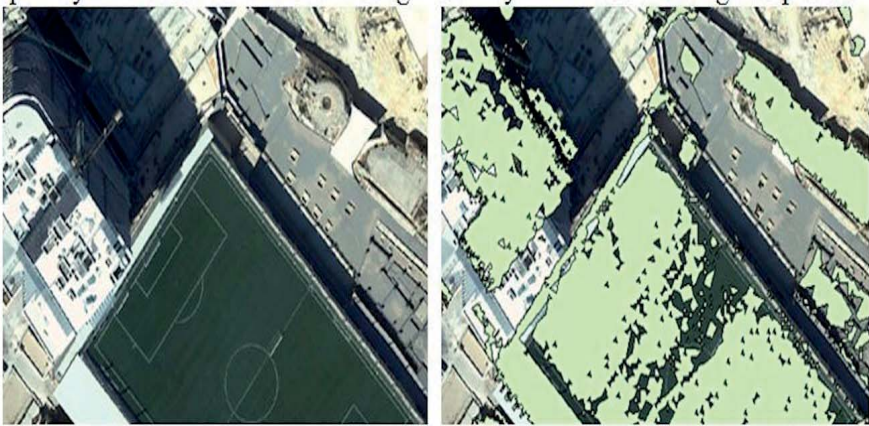
The Maltese rural landscape is typified by centuries old rubble walls that divide and terrace the agricultural land. In more than a few cases these old walls have a thickness of a metre or more. These features posed a problem when extracting building footprints from the LiDAR data because they were selected with the building features. Since these thick rubble walls are constructed from the same fabric they share the same intensity value range as stone buildings. The issue is compounded by the fact that long networks of thick rubble walls have a large surface area and cannot be selected and eliminated by a minimum area without also selecting and eliminating legitimate building footprints. By the same token boats and larger vehicles were not always eliminated because the objects had an area larger than small buildings. This issue required manual or semi-automatic processing by only selecting building footprints within development and urban zones, within coastal boundaries and eliminating objects within road polygons.

Figure 10: Gudja showing thick rubble walls selected with building features



A facet of urban landscape that caused problems was roof gardens, roof level vegetation, and roof-top sports grounds with artificial turf; because when urban vegetation was eliminated by filtering on intensity values, the buildings with vegetation at roof level were also selected. Thus these features were either completely eliminated or resulted in significantly distorted building footprints.

Figure 11: Sliema showing difficulty in extracting building footprint of turf covered rooftop



## Conclusion

The results from the areas that have higher urban development, such as Sliema and Mosta in these trials, show that this process is well suited to identifying the building footprints themselves. This is mainly due to the fact that there is less contrast in the landscape and surrounding features. While in the more rural areas the buildings have very similar characteristics to the rest of the landscape making the extraction of the building footprint less straightforward. Rural areas tend to be largely less developed in terms of building heights and overall volume of the buildings, besides having thick rubble walls that have very similar intensity values to the building features in these areas. Therefore, removal of the rubble walls during the extraction process is more complicated. In some cases, ploughed fields within the rural areas also often displayed similar intensity values to the rubble walls and buildings themselves. This is unlike the vegetated areas within the more urban areas that were often greener, possibly due to better irrigation, rendering the intensity filtering and the removal of the vegetation slightly simpler. On the other hand in the urbanised areas garden rooftops that contain vegetation did cause some extraction issues when filtering by attributes such as intensity. Therefore identifying a specific value range was required. This then allowed removal of large areas of vegetation without having a great detrimental effect on building footprints on building features with rooftop garden.

Creating a filtered TIN and non-filtered TIN allowed the separation of ground points and non-ground points retaining, besides the building features, extra unwanted objects such as cars, large vehicles, boats and vegetation. However, attributes such as area proved very useful in this method by filtering out cars based on the surface area of the average

sized car. Filtering by area values did not completely eliminate other features such as rubble walls in the rural areas, even though the filtering values were increased slightly in the rural area, the values could not be increased greatly as increases by too large a value would potentially lead to the removal of footprints of smaller buildings.

From these trials it can be concluded that it is quick and easy to produce building footprints from LiDAR point cloud data. The method used here does produce a relatively complete building dataset, however this data cannot be used as a simple replacement to updating building features captured at large-scale. This is because the shape, detail and positional accuracy are not enough to satisfy the specifications of topographic mapping at scales of 1:2500 or larger. However the output can be useful at scales smaller than 1:2500. Further investigation of how this process can be improved is warranted since building edges are a crucial element in large-scale building footprints. One avenue of investigation that could potential enhance the process described in this paper is by classifying and extracting building features from aerial imagery (Yong & Huayi, 2008). These results combined with the outputs from this research could potentially improve the accuracy and shape of the building footprints extracted from LiDAR.

The data would still require some manual manipulation to render the output aesthetically pleasing and to correct inadvertent omissions. Also, additional datasets, like urban development limits, coastal outlines and roads, will be required to filter out features such as thick rubble walls, cars and boats that seep through the extraction process and clutter the building footprint dataset.

The methods for building footprint generation and extraction have to take into consideration the differing landscape and terrain the point cloud data is depicting. In this case if the LiDAR surveys are carried out during the winter/spring periods in the Mediterranean, when the vegetation is the greenest, the intensity mapping and filtering out of vegetation would be facilitated due to higher contrast and higher intensity rates. All in all the results from these trials were rather promising; however it has to be borne in mind that the processes are not totally automatic and do not eliminate all manual intervention. The processes might not be as labour intensive as photogrammetric capture, but the results are also not as sharp and accurate as photogrammetric capture, especially at larger scales. However, these results are promising enough to be considered as an option for a quick and cheap system to detect change in building footprints and urban areas, and as an update at median scales.

## References

- Alexander, C., Smith-Voysey, S., Jarvis, C. & Tansey, K. (2009). Integrating building footprints and LiDAR elevation data to classify roof structures and visualise buildings Computers. *Environment and Urban Systems*, 33, 285-292.
- Alexander, C., Tansey, K., Tate, N., Smith-Voysey, S. & Kaduk, J. (2008). *Extraction of vegetation for topographic mapping from full-waveform airborne laser scanning data*. Paper Presented at: SilviLase. Edinburgh, UK, 17th-19th September, 2008.
- Awrangjeb, M., Ravanbakhsh, M. & Fraser, C. (2010). Automatic detection of residential buildings using LIDAR data and multispectral imagery. *ISPRS Journal of Photogrammetry and Remote Sensing*, 65, 457-467.
- Elashker, A. & Bethel, J. (2002). *Building Extraction Using LiDAR Data*. Paper presented at: ASPRS-ACSM Annual Conference and FIG XXII Congress. Denver, Colorado, 10th-15th November, 2002.
- Goepfer, J., Soergel, U., Heipke, C. & Brzank, A. (2008). An approach for filtering LiDAR data in coastal vegetated areas using intensity information and multiple echoes. *Photogrammetry, Remote Sensing and Spatial Information Sciences*, 37 (B3b), 219-226.
- Goepfert, J., Soergel, U., & Brzank, A. (2008). Integration of intensity information and echo distribution in the filtering process of LiDAR data in vegetated areas. *SilviLaser* (8). Edinburgh, UK. 17th-19th September. Hill, R.
- Haithcoat, T., Song, W. & Hipple, J. (2001). *Automated Building Extraction and Reconstruction from LiDAR Data*. Geographic Resources Centre. Available at: <http://www.grc.missouri.edu/icrestprojarchive/NASA/FeatureExtraction-Buildings/REPYear2-build-extraction.pdf> (accessed on 16 January 2014)
- Hill, J., Graham, L. & Henry, R. (2000). Wide-Area Topographic Mapping and Applications Using Airborne Light Detection and Ranging (LIDAR) Technology. *Photogrammetric Engineering & Remote Sensing*, 66 (8), 908-914.
- Jensen, J. & Cowen, D. (1999). Remote Sensing of Urban/Suburban Infrastructure and Socio-Economic Attributes. *Photogrammetric Engineering & Remote Sensing*, 66(5), 611-622.
- Kim, K. & Shan, J. (2011). *Building footprints extraction of dense residential areas from LiDAR data*. Paper Presented at: ASPRS 2011 Annual Conference. Milwaukee, Wisconsin, 1st-5th May, 2011.

Kwak, E. & Habib, A. (2013). Automatic representation and reconstruction of DBM from LiDAR data using Recursive Minimum Bounding Rectangle. *Journal of Photogrammetry and Remote Sensing*, 285-290.

Ma, R. (2005). DEM Generation and Building Detection from Lidar Data. *Photogrammetric Engineering & Remote Sensing*, 71 (7), 847-854.

Ordnance Survey. (2005). *OS Mastermap: User Guide, Product Specification*. Southampton: Ordnance Survey.

Priestnall, G., Jaafar, J. & Duncan, A. (2000). Extracting urban features from LiDAR digital surface models. *Computers, Environment and Urban Systems*, 24, 65-79.

Shan, J. & Sampath, A. (2005). Urban DEM Generation from Raw Lidar Data: A Labeling Algorithm and its Performance. *Photogrammetric Engineering & Remote Sensing*, 71(2), 217-226.

Shiravi, S., Zhong, M. & Beykaei, S. (2012). *Accuracy assessment of building extraction using LiDAR data for urban planning/transportation applications*. Paper Presented at: Conference of the Transportation Association of Canada. Fredericton, New Brunswick, 14th October, 2012.

Shirowzhan, S. & Lim, S. (2013). *Extraction of Polygon Footprints from LiDAR Data in an Urban Environment*. International Conference on Sustainable Design, Engineering, and Construction. Fort Worth, Texas, 7th-9th November 2012. Chong, W. Place of Publication American Society of Civil Engineers, 246-251.

Thuy Vu, T., Yamazaki, F. & Matsuoka, M. (2009). Multi-Scale Solution for building extraction from LiDAR and image data. *International Journal of Applied Earth Observation and Geo-information*, 11, 281-289.

Wang, O., Lodha, S. & Helmbold, D. (2006). *A Bayesian Approach to Building Footprint Extraction from Aerial LIDAR Data*. 3D Data Processing, Visualization, and Transmission, Third International Symposium. Chapel Hill, North Carolina. 14-16 June, 2006.

Yong, L. & Huayi, W. (2008). Adaptive building edge detection by combining LiDAR data and aerial images. *The internal archives of the photogrammetry, remote sensing and spatial information sciences*, 37, 197-202.

Zhou, Q-Y. & Neumann, U. (2013). Complete residential urban area reconstruction from dense aerial LiDAR point clouds. *Graphical Models*, 75, 118-125.